Acta Cryst. (1993). B49, 6–11

High-Pressure Single-Crystal Structure Study on Calaverite, $AuTe_2$

BY K. REITHMAYER

Institut für Kristallographie und Mineralogie der Universität, Theresienstrasse 41, *D*-8000 *München* 2, *Germany*

W. STEURER

Institut für Mineralogie der Universität, Welfengarten 1, *D*-3000 *Hannover* 1, *Germany*

H. SCHULZ

Institut für Kristallographie und Mineralogie der Universität, Theresienstrasse 41, *D*-8000 *München* 2, *Germany*

AND J. L. DE BOER

Materials Science Centre, Department of Inorganic Chemistry, Nijenborgh 16, *NL*-9747 *AG Groningen, The Netherlands*

(*Received* 27 *May* 1992; *accepted* 2 *July* 1992)

Abstract

Incommensurately modulated calaverite, $AuTe_2$, superspace group $P^{C}_{1}^{2/m}_{s}[-0.41,0,0.45]$, $a = 7.189$ (2), $b = 4.407$ (1), $c = 5.069$ (1) Å, $V = 160.6$ (1) Å^3, $\beta = 89.96$ (2)°, $Z = 2$, $D_x = 9.31$ g cm^{-3}, $F(000) = 366$, μ(Mo $K\alpha$) = 650 cm^{-1}, undergoes a reversible first-order phase transformation at 2.50 (8) GPa. The high-pressure phase, space group $P\bar{3}m1$ (No. 164), is closely related to the CdI_2 structure type. No further phase transformations were observed up to 5.13 GPa. Structure refinements were performed on intensity data collected at 0.05, 0.41, 0.63, 1.63, 1.89, 2.4, 3.09, 3.72 and 5.13 GPa under hydrostatic conditions employing diamond-anvil cells. The coherence length of the modulation decreases with increasing pressure.

Introduction

Calaverite belongs to the group of gold–silver tellurides with chemical formula $Au_{1-x}Ag_xTe_2$. It forms solid solutions with silver up to $x = 0.15$. For $0.20 \leq x \leq 0.28$ the mineral krennerite is formed; the mineral sylvanite is stable for $x \simeq 0.50$. All three minerals belong to different structure types (Tunell & Pauling, 1952; Van Tendeloo, Gregoriades & Amelinckx, 1983; Van Tendeloo, Amelinckx & Gregoriades 1984; Schutte & de Boer, 1988). The average structure of calaverite may be described as a distorted CdI_2 structure. The Te atoms form a strongly distorted hexagonal close packing with half of the octahedral voids filled by the cations. Thus, the structure consists of layers of distorted $AuTe_6$ octahedra with two Au–Te distances of 2.673 (2) and four of 2.971 (2) Å.

Table 1. *Data-collection parameters*

P: pressure; *N*: measured reflections; N_R: rejected reflections; N_U: unique reflections; R_I: *R* value of internal consistency of equivalent reflections. Values in parentheses: data for trigonal reindexed data sets. Pressure uncertainty: 0.08 GPa.

P (GPa)	*N*	N_R	N_U	$(\sin\theta)/\lambda$ (Å^{-1})	R_I
0.0001	770	–	425	0.83	0.064
< 0.05	368	2	139	0.81	0.055
0.41	295	6	138	0.70	0.052
0.63	368	3	138	0.81	0.069
1.63	356	7	119	0.81	0.043
1.78	441	130	205	0.70	0.048
1.89	345	11	111	0.81	0.060
2.40	344	2	155	0.81	0.060
3.09	336	3	159 (99)	0.81	0.038 (0.043)
3.72	338	3	160 (101)	0.81	0.040 (0.044)
5.13	333	2	156 (99)	0.81	0.043 (0.050)
0.0001*	2179	–	1130	0.83	0.075
1.78*	1220	292	551	0.70	0.059

*Data sets including satellite reflections.

Calaverite is one-dimensionally incommensurately modulated. The modulation is of the displacive type and in the case of the silver-containing calaverite it is accompanied by a density modulation. The displacive part of the modulation mainly affects the Te atoms, which display a large amplitude of about 0.4 Å parallel to **b**. The Au atoms show only small amplitudes. The probability of their substitution by silver is provided for by the density-modulation function. The modulation gives rise to strong satellite reflections, which can be measured up to the third order (Schutte & de Boer, 1988). Calaverite was the first incommensurate phase found with clearly defined satellite crystal faces (Dam, Janner & Donnay, 1985; Janner & Dam, 1989).

0108-7681/93/010006-06$06.00

In a high-pressure single-crystal experiment carried out on silver-free calaverite a reversible nonquenchable first-order phase transformation was detected (Reithmayer, Steurer, Schulz & de Boer, 1990). Since the high-pressure phase was preserved as a single crystal, it was possible to examine its structure *in situ* by means of X-ray diffraction techniques. Also the structural changes at pressures below the phase transformation were of interest. These measurements were analysed in terms of the average structures; the modulated structures, including first-order satellite reflections were also determined for 0.05 (8) and 1.78 (8) GPa.

Experimental

Crystals of $AuTe_2$ were grown by both the Kyropoulos and the Bridgman methods. For the experiments, the higher-quality crystals obtained by the latter method were used. Small crystal spheres were prepared with diameters of about 40 to 60 μm to simplify the absorption correction.

The data sets of main reflections of the low- and high-pressure phases were collected with a gasketed diamond-anvil cell of Merrill–Bassett type (Merrill & Bassett, 1974). Before a 270 μm sample-chamber hole was drilled by spark erosion, the gasket (Inconel 718 steel) was preindented by the diamond anvils to a thickness of about 120 μm. The spherical $AuTe_2$ crystals were mounted into the sample chamber together with a small ruby crystal for pressure calibration (Piermarini, Block, Barnett & Forman, 1975). The crystals were fixed on the diamond faces by a thin film of silicon grease.

The data sets including first-order satellite reflections were collected with a diamond-anvil cell of the MPI-Stuttgart type (Köpke & Schulz, 1986). The gasket material was I-70 beryllium from the Brush–Wellman company. To maintain hydrostatic conditions a mixture of methanol and ethanol (ratio 4:1; Piermarini, Block & Barnett, 1973) was used.

All data collections were performed on an Enraf–Nonius CAD-4 four-circle single-crystal diffractometer with graphite-monochromatized Mo $K\alpha$ radiation. Table 1 gives a survey of the experiments: intensity data sets were collected at ambient pressure and at < 0.05 (8), 0.41 (8), 0.63 (8), 1.63 (8), 1.78 (8), 1.89 (8), 2.40 (8), 3.09 (8), 3.72 (8) and 5.13 (8) GPa; additionally, the lattice parameters were measured at pressures of 0.05 (8), 0.21 (8), 1.03 (8), 2.63 (8) and 4.12 (8) GPa. For the experiments employing the Merrill–Bassett-type cell a special diffractometer-control program was used (Finger & King, 1978).

Because of the special geometry of the MPI cell, about 90% of one hemisphere in reciprocal space is accessible in a data collection, *i.e.* nearly all of the reflections with negative χ. Thus a reflection list was calculated containing all main and satellite reflections with $0 \geq \chi \geq -100°$ and $0 \leq \theta \leq 40°$. Consequently, this type of diamond-anvil cell does not allow the measurement of Friedel pairs except at a χ value of about 0°. The profiles of the satellite reflections were measured at a pressure of 1.81 (8) GPa on the five-circle diffractometer at HASYLAB, Hamburg, Germany (Kupcik, Wendschuh-Josties, Wolf & Wulf, 1986) using synchrotron radiation.

All data sets have been corrected for the absorption caused by the respective diamond-anvil cell. To account for the absorption inside the crystals ($1.3 \leq \mu r \leq 2$), spherical-absorption corrections were applied. The least-squares refinements of the modulated structure were performed with the program *REMOS*82.0 (Yamamoto, 1982), those of the average structures with the program *PROMETHEUS* (Zucker, Perenthaler, Kuhs, Bachmann & Schulz, 1983).* In the calculations an isotropic temperature factor for Au, the x and z coordinates and a constrained anisotropic temperature factor (rotational ellipsoid) for Te, a parameter accounting for secondary extinction and a scale factor were refined. The anisotropic temperature factor for Te had to be constrained anisotropic temperature factor (rotational ellipsoid) for Te, a parameter accounting for sity data in particular directions of the reciprocal space to a considerable amount. Unconstrained refinements, consequently, would result in biased anisotropic thermal parameters. At 1.78 GPa, using the MPI cell, it was possible to refine the modulated structure and the average structure with unconstrained anisotropic temperature factors for both Te and Au atoms. The high-pressure phase could also be refined with unconstrained anisotropic temperature factors in both space groups. At pressures below the phase transformation the existence of an additional correlation between the modulation amplitude along **b** and the temperature coefficients of the other main directions became evident. The R factors used were

$$wR = [\sum w(|F_{obs}| - |F_{calc}|)^2 / \sum wF_{obs}^2]^{1/2}$$

and

$$R = \sum(|F_{obs}| - |F_{calc}|) / \sum|F_{obs}|$$

with weights $w = 1/\sigma^2(F)$.

Results and discussion

At pressures up to the phase transformation the lattice parameters show a very anisotropic behaviour. While a exhibits a small nonlinear

* Lists of structure factors at the above-mentioned pressures have been deposited with the British Library Document Supply Centre as Supplementary Publication No. SUP 55482 (37 pp.). Copies may be obtained through The Technical Editor, International Union of Crystallography, 5 Abbey Square, Chester CH1 2HU, England.

decrease, c decreases linearly, but both decrease less than 0.1 Å. In contrast, b becomes about 0.3 Å smaller. β increases with pressure up to 90.42 (4)°. Above the transformation pressure a, b and c change linearly while β remains at 90°. The scattering of the values for β (Fig. 1) around 90° at different pressures can be explained by a slight misalignment of the crystal in the high-pressure cell. The ratio a/b above the transformation is $3^{1/2}$. This is the ratio which would be obtained in the case of an orthohexagonal setting.

How does the structue of $AuTe_2$ change as more and more pressure is applied to the crystal? In the average structure, the atoms occupy the following Wyckoff positions: Au in 2(a), (0,0,0), Te in 4(i), (x,0,z), $x = 0.6883$ (3), $z = 0.2881$ (4). There is no possibility for atoms to move along the c direction for steric reasons. Thus, the relative z coordinate of Te increases at the same rate as the c lattice parameter decreases to maintain a constant distance of 1.462 (3) Å of Te atoms to the (001) plane. The same is also true for the high-pressure phase. With increasing pressure, the x coordinate of Te approximates a value of $\frac{2}{3}$ (compare Table 2), locking into this value at the phase transformation (Fig. 2). As already mentioned above, b decreases by about 0.3 Å while the y coordinates of all atoms in the average structure are zero for all pressures. Thus, the compression

Table 2. *Structure data of the phase below the transformation (without data for the modulated phase)*

Values in parentheses are e.s.d.'s. Pressure uncertainty: 0.08 GPa.

		<0.05 GPa	0.41 GPa	0.63 GPa	1.63 GPa	1.89 GPa	2.40 GPa
Au	x	0	0	0	0	0	0
	y	0	0	0	0	0	0
	z	0	0	0	0	0	0
	U	0.0132 (8)	0.0146 (15)	0.0114 (7)	0.0132 (6)	0.0137 (6)	0.0111 (7)
Te	x	0.6879 (5)	0.6875 (5)	0.6871 (5)	0.6840 (8)	0.6826 (7)	0.6773 (4)
	y	0	0	0	0	0	0
	z	0.2889 (13)	0.2887 (9)	0.2897 (12)	0.2907 (6)	0.2915 (5)	0.2914 (8)
	u	0.012 (2)	0.011 (2)	0.011 (2)	0.0087 (8)	0.0109 (7)	0.019 (2)
	u_{22}	0.100 (3)	0.076 (7)	0.086 (3)	0.068 (3)	0.060 (1)	0.037 (2)
R		0.088	0.084	0.071	0.063	0.049	0.058
wR		0.053	0.058	0.052	0.042	0.035	0.049

of the structure along the b direction is connected with a shortening of the modulated Au–Te bond lengths. An indirect measure for this is the decrease of the coefficient u_{22} of the anisotropic temperature factor (Fig. 3). u_{22} returns to normal values in the high-pressure structure. To understand the structural changes, the Au–Te and Te–Te distances were plotted *versus* pressure (Fig. 4). A schematic representation of distances of the different atoms is given in Fig. 5. The Au–Te bonds show a decrease of the longer bond [Au–Te($B1$–$B4$)] with increasing pressure, accompanied by a slow increase of the shorter distance [Au–Te($A1$,$A2$)]. In the high-

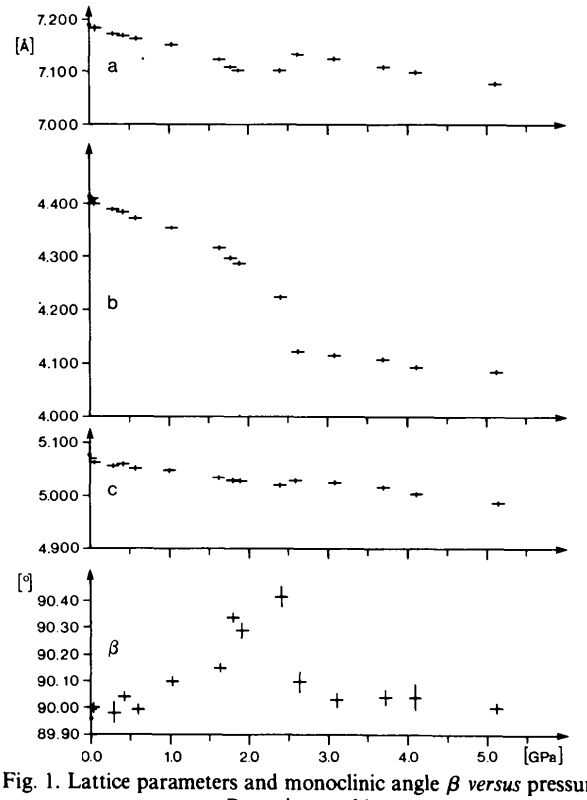

Fig. 1. Lattice parameters and monoclinic angle β *versus* pressure. Bars give e.s.d.'s.

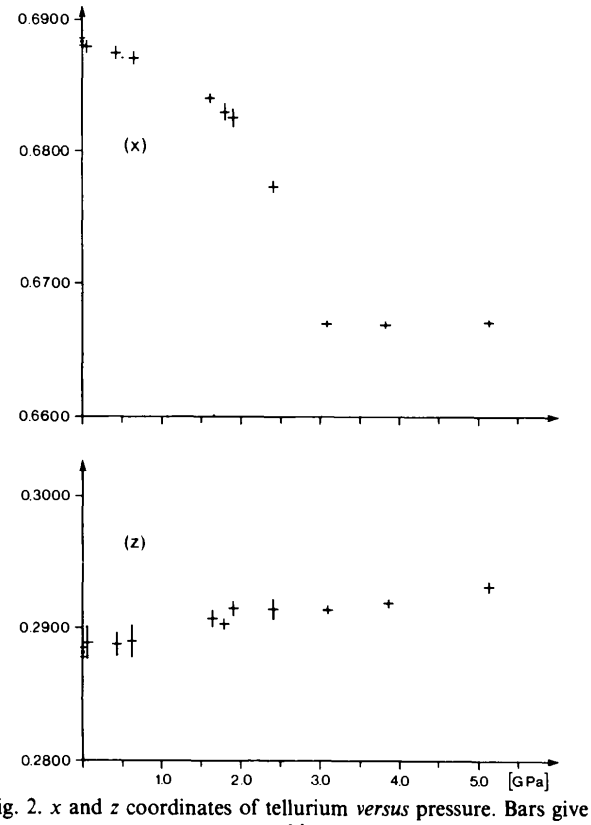

Fig. 2. x and z coordinates of tellurium *versus* pressure. Bars give e.s.d.'s.

pressure phase only one bond length exists between Au and Te. An examination of the various Te–Te distances gives the following picture: Te–Te(1,3) and Te–Te(2) both decrease while in the high-pressure phase they are of the same length. Te–Te(5,6) and a new neighbour atom, Te–Te(4), also tend to a common distance that is reached in the high-pressure phase. The breaking of the close Au–Te bond explains the increase of the *a* and *c* lattice parameters at the phase transformation. The increasing short Au–Te distance of the octahedra also increases the *a* and *c* axes. The Te atoms of the anion layers glide into a more symmetrically coordinated geometrical position (Fig. 6).

The phase transformation can be characterized by both displacive and reconstructive elements. With increasing pressure the $AuTe_6$ octhedra exhibit a small tilt of less than 1.5° towards to the *ab* plane. At

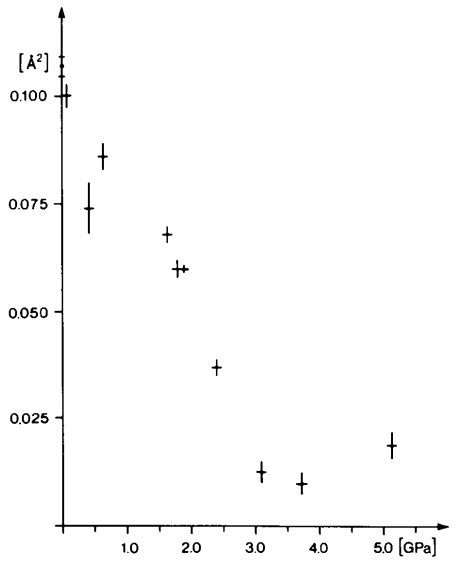

Fig. 3. Coefficient u_{22} of the anisotropic temperature factor of tellurium *versus* pressure. Bars give e.s.d.'s.

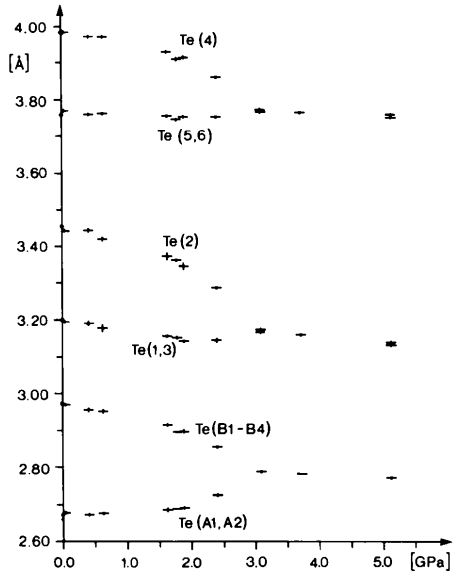

Fig. 4. Bond lengths between Au and Te as well as bond lengths Te–Te(1,3), Te–Te(2), Te–Te(4) and Te–Te(5,6) in the average structure. For atom numbering refer to Fig. 5. Bars give e.s.d.'s.

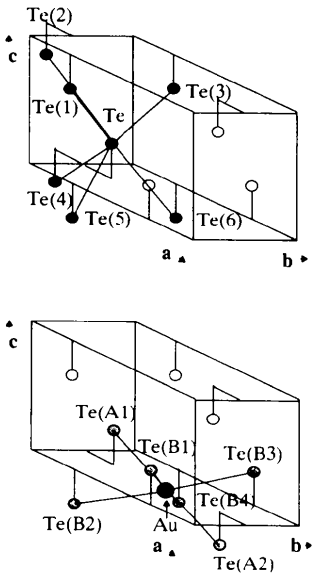

Fig. 5. Schematic drawings of the coordination of gold and tellurium.

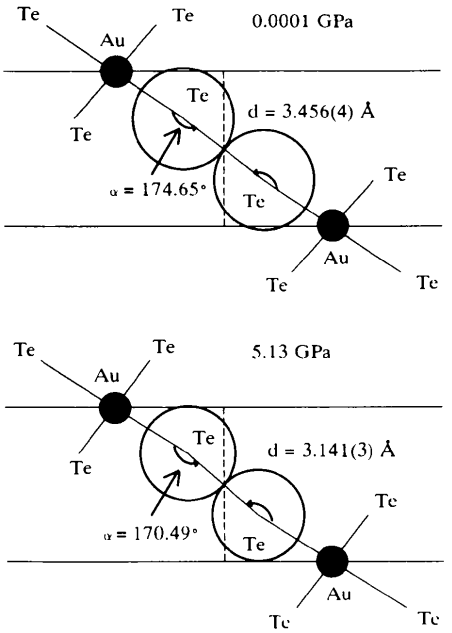

Fig. 6. Magnified projection of two adjacent octahedra parallel to **b**. The conditions are shown at 0.0001 and 5.13 GPa. The geometrical lock-in of the Te atoms is clearly seen. *d* is the Te–Te(2) distance.

Table 3. *Structure data of the high-pressure phase*

Values in parentheses are e.s.d.'s. Pressure uncertainty: 0.08 GPa.

		3.09 GPa	3.72 GPa	5.13 GPa
Au	x	0	0	0
	y	0	0	0
	z	0	0	0
	u_{11}	0.0124 (7)	0.0129 (7)	0.0117 (9)
	u_{22}	0.0124 (7)	0.0129 (7)	0.0117 (9)
	u_{33}	0.0142 (4)	0.0125 (9)	0.0074 (15)
	u_{12}	0.0062 (4)	0.0064 (3)	0.0059 (4)
Te	x	$\frac{1}{3}$	$\frac{1}{3}$	$\frac{1}{3}$
	y	$\frac{2}{3}$	$\frac{2}{3}$	$\frac{2}{3}$
	z	0.2913 (3)	0.2919 (3)	0.2932 (4)
	u_{11}	0.0148 (7)	0.0144 (7)	0.0105 (8)
	u_{22}	0.0148 (7)	0.0144 (7)	0.0105 (8)
	u_{33}	0.0148 (13)	0.0128 (12)	0.0104 (19)
	u_{12}	0.0074 (4)	0.0072 (4)	0.0052 (4)
R		0.043	0.041	0.055
wR		0.030	0.028	0.027

the phase transformation a discontinuity of about 0.8° of the tilt angle occurs and above the transformation the tilt angle slowly increases. A reconstructive element is the increase of the number of chemically equivalent atoms in the first coordination shell of tellurium from five to six. Above the phase-transformation pressure the distances of all atoms show the normal interatomic bond lengths one would expect under these conditions.

At pressures above the phase transformation no satellite reflections could be observed. The coefficient u_{22} of tellurium shows normal values. It can be concluded that the modulation has vanished in the high-pressure phase. The atomic positions in the monoclinic unit cell of the high-pressure phase could be easily identified in the space group $P\bar{3}m1$. Au takes the position of Cd, 1(*a*), (0,0,0), Te that of I, 2(*d*), ($\frac{1}{3}$,$\frac{2}{3}$, z). To verify the symmetry of the high-pressure structure, Hamilton tests (Hamilton, 1965) on the significance of the weighted R values were performed. The results showed a preference for the CdI_2 structure with space group $P\bar{3}m1$. Table 3 shows the refinement results for the high-pressure phase at different pressures. Because of the very small a/c ratio (about 1.22 in comparison to an ideal ratio of 1.633) the structure represents a distorted CdI_2 structure. This, of course, does not affect the symmetry of the high-pressure phase.

An unsolved problem remains the question of which valence states Te and Au might adopt in $AuTe_2$. Schutte & de Boer (1988) proposed the model of a valence fluctuation between Au^+ and Au^{3+} to explain the modulation. Meanwhile, X-ray photoelectron spectrocopy measurements showed a single valence state for Au (van Triest, Folkerts & Haas, 1990). We propose for the high-pressure phase a separation of metallic bond states between Au and Te and strong covalent bonds between neighbouring Te atoms. This could be deduced from examination of the bond lengths. The bonds between Au and Te of the high-pressure phase display lengths typical of intermetallic bonds. The closest distances between Te atoms are not so small as in Te crystals (about 2.82 Å) (Cherin & Unger, 1967), but there are comparable properties in the two types of crystals.

Table 4. *Structure data of the modulated phase at* 0.0001 *and* 1.78 GPa

Values in parentheses give e.s.d.'s. First-order satellite reflections only allow the refinement of the y components of the modulation function used $A(\mathbf{q}.\mathbf{r}) = a_1^c\cos(\mathbf{q}.\mathbf{r}) + a_1^s\sin(\mathbf{q}.\mathbf{r})$. Pressure uncertainty: 0.08 GPa.

	P (GPa)		$A(0)$	a_1^c	a_1^s
Au	0.0001	x	0	–	–
		y	0	0.0057 (4)	–
		z	0	–	–
		u_{11}	0.0152 (5)	–	–
		u_{22}	0.0205 (5)	–	–
		u_{33}	0.0139 (5)	–	–
		u_{13}	0.0020 (2)	–	–
Te		x	0.6884 (2)	–	–
		y	0	0.0007 (7)	0.0837 (6)
		z	0.2878 (3)	–	–
		u_{11}	0.0167 (5)	–	–
		u_{22}	0.0103 (13)	–	–
		u_{33}	0.0104 (5)	–	–
		u_{13}	0.0017 (4)	–	–
Au	1.78	x	0	–	–
		y	0	0.0016 (6)	–
		z	0	–	–
		u_{11}	0.0130 (8)	–	–
		u_{22}	0.0180 (7)	–	–
		u_{33}	0.0126 (9)	–	–
		u_{13}	0.0043 (4)	–	–
Te		x	0.6832 (1)	–	–
		y	0	−0.0043 (13)	0.0640 (18)
		z	0.2903 (3)	–	–
		u_{11}	0.0161 (10)	–	–
		u_{22}	0.0156 (26)	–	–
		u_{33}	0.0105 (10)	–	–
		u_{13}	0.0051 (7)	–	–

Table 5. *R values for main and satellite reflections*

(MR): main reflections; (SR): satellite reflections; R, wR: overall R values.

P (GPa)	R(MR)	wR(MR)	R(SR)	wR(SR)	R	wR
0.0001	0.053	0.060	0.198	0.175	0.100	0.085
1.78	0.047	0.048	0.169	0.142	0.084	0.059

For the first time a data collection of main and satellite reflections of a modulated crystal under high pressure was performed to carry out a higher-dimensional structure analysis. The behaviour of the modulated phase under pressure was investigated at 1.78 (8) GPa. To compare the structural changes, an additional data set including first-order satellites was measured at ambient conditions. The refinement with *REMOS*82.0 (Yamamoto, 1982) allows the separation of thermal and modulational parameters, which are mixed in the average structure. The refined data are given in Tables 4 and 5. The separation of the coefficients of the modulation wave and the anisotropic temperature factor clearly shows the decrease of the modulation amplitude of the Te atoms. Another interesting subject was the examination of selected profiles of satellite reflections under pressure. For better resolution synchrotron radiaton was used. Comparison with the profiles of an identical second crystal at ambient conditions revealed a significant broadening of the reflections under pressure. This can be seen as a decrease of coherence length of the

modulation function. Together with the decreasing amplitude of the atoms this points towards an ordinary crystal structure, which is reached at the transformation point.

This phase transformation is a further example of incommensurate–commensurate transformations. The strong variation of the reflection intensities with pressure allowed an accurate examination of the changing structural properties under high pressure. For further investigations it would be interesting to examine the influence of silver on the phase transformation.

This work was supported by the Bundesminister für Forschung und Technologie, grant No. 05 464 IBB9.

References

CHERIN, P. & UNGER, P. (1967). *Acta Cryst.* **23**, 670–671.
DAM, B., JANNER, A. & DONNAY, J. D. H. (1985). *Phys. Rev. Lett.* **55**, 2301–2304.
FINGER, L. W. & KING, H. (1978). *Am. Mineral.* **63**, 337.
HAMILTON, W. C. (1965). *Acta Cryst.* **18**, 502–510.
JANNER, A. & DAM, B. (1989). *Acta Cryst.* A**45**, 115–123.
KÖPKE, J. & SCHULZ, H. (1986). *Phys. Chem. Miner.* **13**, 165–173.
KUPCIK, V., WENDSCHUH-JOSTIES, M., WOLF, A. & WULF, R. (1986). *Nucl. Instrum. Methods*, A**246**, 624–626.
MERRILL, L. & BASSETT, W. A. (1974). *Rev. Sci. Instrum.* **45**, 290–294.
PIERMARINI, G. J., BLOCK, S. & BARNETT, J. D. (1973). *J. Appl. Phys.* **44**, 5377–5382.
PIERMARINI, G. J., BLOCK, S., BARNETT, J. D. & FORMAN, R. D. (1975). *J. Appl. Phys.* **46**, 2774–2780.
REITHMAYER, K., STEURER, W., SCHULZ, H. & DE BOER, J. L. (1990). *Acta Cryst.* A**46**, C-393–C-394.
SCHUTTE, W. J. & DE BOER, J. L. (1988). *Acta Cryst.* B**44**, 486–494.
TRIEST, A. VAN, FOLKERTS, W. & HAAS, C. (1990). *J. Phys. Condens. Matter*, **2**, 8733–8740.
TUNELL, G. & PAULING, L. (1952). *Acta Cryst.* **5**, 375–381.
VAN TENDELOO, G., AMELINCKX, S. & GREGORIADES, P. (1984). *J. Solid State Chem.* **53**, 281–289.
VAN TENDELOO, G., GREGORIADES, P. & AMELINCKX, S. (1983). *J. Solid State Chem.* **50**, 321–334, 335–361.
YAMAMOTO, A. (1982). *REMOS*82.0. *Computer Program for the Refinement of Modulated Structures.* National Institute for Research in Inorganic Materials, Sakura-mura, Niihari-gun, Ibaraki 305, Japan.
ZUCKER, U., PERENTHALER, E., KUHS, W. F., BACHMANN, R. & SCHULZ, H. (1983). *J. Appl. Cryst.* **16**, 358.

Acta Cryst. (1993). B**49**, 11–18

Thermal Vibrations of Atoms and Phase Transition in $RbHSeO_4$ and NH_4HSeO_4 Single Crystals

BY I. P. MAKAROVA

Institute of Crystallography, Academy of Sciences, Leninsky pr. 59, 117333 *Moscow, Russia*

(*Received* 16 *January* 1992; *accepted* 5 *June* 1992)

Abstract

Using neutron diffraction data on single crystals of $RbHSeO_4$ in the paraelectric phase at 383 K and in the ferroelectric phase at 293 K, and NH_4HSeO_4 crystals in the paraelectric phase at 293 and 400 K, the thermal vibration parameters of the atoms in these crystals as well as the structural changes in $RbHSeO_4$ during the ferroelectric phase transition have been studied. The phase transitions in these crystals are due to ordering of the H-atom arrangement for one of the hydrogen bonds.

Introduction

Similar sequences of phase transitions have been found in $RbHSeO_4$ and NH_4HSeO_4 crystals (Poprawski, Mroz, Czapla & Sobczyk, 1979; Czapla, Lis & Sobczyk, 1979; Rozanov, Moskvitch, Sukhovsky & Aleksandrova, 1983; Czapla, 1982; Suzuki, Osaka & Makita, 1979; Moskvitch, Sukhovsky & Rozanov, 1984; Aleksandrova, Blat, Zinenko, Moskvitch & Sukhovsky, 1987). Replacement of the Rb atom by the $[NH_4]$ group lowers the ferroelectric phase transition temperature by 120 K (from 370 to 250 K) (Poprawski, Mroz, Czapla & Sobczyk, 1979; Czapla, Lis & Sobczyk, 1979). X-ray structural studies of the paraelectric and ferroelectric phases provide reliable information on the heavy atoms (Waśkowska, Olejnik, Łukaszewicz & Czapla, 1980; Waśkowska, Olejnik, Łukaszewicz & Głowiak, 1978; Aleksandrov, Kruglik, Misul & Simonov, 1980; Kruglik, Misul & Aleksandrov, 1980) and show that the corresponding phases of these crystals are isostructural. The accuracy of the X-ray diffraction data was however insufficient to locate the H atoms and to study the changes in the hydrogen bonds during the phase transitions. NMR data on ^{77}Se suggested that the ferroelectric phase transition in these crystals is due

0108-7681/93/010011-08$06.00